2012 Fourth International EURASIP Workshop on RFID Technology

Evaluating On-Body RFID Systems at 900 MHz and 2.45 GHz

Jasmin Grosinger and Michael Fischer
Vienna University of Technology
Institute of Telecommunications
Vienna, Austria
jgrosing@nt.tuwien.ac.at

***Abstract*—This contribution evaluates backscatter radio frequency identification (RFID) systems on the body of a human being at 900 MHz and 2.45 GHz. The systems are composed of different on-body antennas. Custom-built monopole antennas act as a best-case reference, while less efficient patch antennas are used to give an insight in practical system implementations. The evaluation of these systems is based on channel transfer function measurements, which allows to deduce outage probabilities of the RFID systems. These probabilities give an insight in the system performance in forward and backward link and help to identify the limitations in the backscatter communication to realize a reliable system.**

***Keywords*-backscatter radio frequency identification (RFID), on-body RFID system, on-body antenna, system evaluation, outage probability**

I. Introduction

Wireless body area networks (WBANs) enable many new promising applications in the field of remote health monitoring, therapy support at home, wellness, and fitness [1], [2]. These networks connect independent nodes, e.g., sensors situated in clothes, on the body, or under the skin of a person, through a wireless communication channel.

A promising communication technology for WBANs is backscatter radio frequency identification (RFID) in the ultra high frequency (UHF) range [3]. Backscatter RFID relies on the radio communication between an RFID reader, acting as a control unit, and a multitude of passive or semi-passive RFID transponders, acting as sensor nodes. In the forward link, the RFID reader transmits radio frequency power and data to the tag. In the return link, whenever a reader command requires a tag's response, the tag, which consists of an antenna and an integrated circuit chip, starts its data transfer using a modulated backscatter signal [4]. Consequently, backscatter tags have a low power consumption and are suitable for WBANs that require small, light-weight, and low-maintenance devices. Additionally, research efforts are ongoing to integrate sensing capabilities in backscatter tags without enhancing their power consumption [5]–[7]. Such sensor tags can then be used to monitor the physiological parameters of a person, e.g., blood pressure, temperature, heartbeat, body motion. E.g., the backscatter bend sensor proposed in [7], which senses an object's curvature, could be used to monitor the motion sequence of people for sports analysis or for human computer interaction devices when a patient is undergoing physical therapy.

In a backscatter RFID system, it is vital to ensure a power efficient communication [8]. If the power at the tag's chip is smaller than the tag's sensitivity (the minimum power required to power up the tag), the backscatter communication system is limited in its forward link. If the power at the reader receiver is smaller than the receiver's sensitivity, a limitation in the backward link occurs. Thus, to realize a robust power transfer and communication in on-body RFID systems, it is mandatory to investigate the on-body radio propagation channel, including the effects of the antennas, and to evaluate the backscatter performance of the on-body system in a realistic scenario.

Previous research on UHF RFID-based WBANs has focused on in-body [9]–[11] and off-body [12]–[14] communication systems (this classification of WBANs is introduced in [15]). So far, the investigation of backscatter communication systems on the body has received less attention in the literature. A first feasibility study of an on-body backscatter RFID system is presented in [16] and is based on backscatter measurements at $870\,\mathrm{MHz}$. The investigated RFID system consists of a reader with a patch antenna and five on-body tags composed of of custom-built wearable felt antennas. A preliminary performance analysis of an on-body RFID system composed of monopole antennas operating at $900\,\mathrm{MHz}$ is presented in [3]. This contribution extends these evaluations by investigating different on-body RFID systems, each composed of monopole or patch antennas operating at $900\,\mathrm{MHz}$ or $2.45\,\mathrm{GHz}$.

Sec. II describes the investigated on-body RFID systems and their antennas. The performance evaluation of the systems' forward and backward link is presented in Sec. III.

II. On-Body RFID Systems

The arrangement of the RFID reader and tags in the on-body systems, which are investigated, is shown in Fig. 1. The RFID reader is situated on the stomach of an adult female, while four RFID tags are placed at various positions on the female's body: on the right chest, on the middle of the back, on the left side of the head, and on the right wrist. These links represent two trunk-to-trunk, a trunk-to-head, and a

978-0-7695-4813-5/12 $26.00 © 2012 IEEE
DOI 10.1109/RFID.2012.14

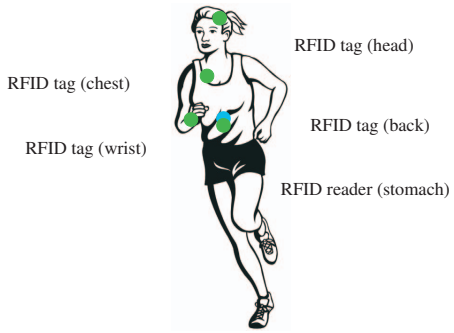

Figure 1. System arrangement of the on-body RFID reader and tags

trunk-to-limb link following a classification of on-body links introduced in [15].

A. Antennas

On-body antennas are influenced by the close proximity of the human body. Proximity effects, which might be experienced by an antenna on the body, include a shift in the antenna's resonant frequency, a distortion of its radiation pattern, and a reduction in its radiation efficiency [17]. The primary requirement for on-body antennas is that the mutual influence between the antenna and the human body is low. This decoupling can be achieved by metallic shields, which are integrated in the antennas as groundplanes [13]. Suitable antenna types are for example monopoles or patch antennas, their groundplanes mounted parallel to the body surface.

1) Monopole Antennas: Practically, a monopole antenna is not suitable for WBAN applications, because it is not low profile. But monopoles show the best performance in WBANs [17], [18]. A monopole shows an omnidirectional radiation pattern on the body, i.e., a maximum radiation along the body's surface. Such a radiation pattern is favorable for on-body links, where the main mechanism for propagation around the body is via a surface wave. Thus, they are used as a best-case reference in this contribution and help to define an upper bound for the performance of practical system implementations.

Monopole antennas resonant at $900\,\mathrm{MHz}$ and $2.45\,\mathrm{GHz}$ were designed by means of a human body model [19] and realized on FR-4 substrate with a thickness of $1.6\,\mathrm{mm}$ [17]. The design was done for an antenna-to-body separation distance of $5\,\mathrm{mm}$. The simulated radiation efficiency of the monopoles operating at $900\,\mathrm{MHz}$ is $77\,\%$, in comparison to the monopole in vacuum, which shows an efficiency of $97\,\%$. The maximum total gain compared to an isotropic radiator is $1.3\,\mathrm{dBi}$ on the body and $2.1\,\mathrm{dBi}$ in vacuum. The monopoles at $2.45\,\mathrm{GHz}$ show a radiation efficiency of $71\,\%$, in comparison to an efficiency of $97\,\%$ in vacuum. The gain is $1.6\,\mathrm{dBi}$ on the body and $2.2\,\mathrm{dBi}$ in vacuum. The smaller efficiency at $2.45\,\mathrm{GHz}$, although the groundplane is bigger than the radiator length in comparison to the $900\,\mathrm{MHz}$ monopole, is due to higher losses in human tissues at higher frequencies [20]. All monopoles are matched to a $50\,\Omega$ feed and show an overall matching of some $-10\,\mathrm{dB}$, which is sufficient for real-world systems. Pictures of the realized monopoles and their dimensions are depicted in Fig. 2.

2) Patch Antennas: Patch antennas are low profile and show a broadside radiation, when they are excited at their fundamental mode, i.e., a maximum radiation away from the body. This radiation characteristic is suitable for on-body links where the propagation path is a free space path or a shadowed free space path with diffraction around the body (e.g., stomach-wrist link) [18]. In addition, there is the possibility to realize patch antennas which work at a higher mode with a maximum radiation along the body's surface [17]. This radiation pattern is suitable for on-body links, where the propagation is predominantly due to a surface wave along the body [18]. Patch antennas are thus suitable for on-body applications. The less efficient patch antennas, in comparison to monopoles, represent practical tag antennas and provide an insight in the performance of practical on-body systems.

In a first attempt, an initial set of patch antennas was designed and realized on FR-4 for the $900\,\mathrm{MHz}$ and $2.45\,\mathrm{GHz}$ regime. Again, the antennas were designed for an antenna-to-body separation of $5\,\mathrm{mm}$. The patch antennas show a broadside radiation. The patch at $900\,\mathrm{MHz}$ shows a simulated radiation efficiency of $22\,\%$ and a peak gain of $-1.2\,\mathrm{dBi}$. In comparison, the patch antenna in vacuum shows an efficiency of $24\,\%$ and a gain of $-0.7\,\mathrm{dBi}$. While the patch antenna for the $2.45\,\mathrm{GHz}$ regime shows a radiation efficiency of $42\,\%$ on the body and of $47\,\%$ in vacuum. The gain is $2.7\,\mathrm{dBi}$ on the body and $3.7\,\mathrm{dBi}$ in vacuum. The higher radiation efficiency in comparison to the patch antenna at $900\,\mathrm{MHz}$ is due to the large size of the groundplane relative to the patch size. Again, the antennas are matched to a $50\,\Omega$ feed and show a matching of some $-10\,\mathrm{dB}$ in the operating frequency range. A picture and the dimensions of the patch antennas can be seen in Fig. 3.

B. Measurement Setup

Each on-body RFID system is composed of monopole or patch antennas operating as both reader and tag antennas. The investigation of the systems is done by means of channel measurements at $900\,\mathrm{MHz}$ and $2.45\,\mathrm{GHz}$. The measurement setup is detailed in [19]. The channel transfer function of the forward link, S_{21}, and the backward link, S_{12}, between the reader antenna on the stomach and the four different tag antennas were captured by means of a vector network analyzer. These functions were measured versus standing, sitting, and walking body postures in an indoor scenario.

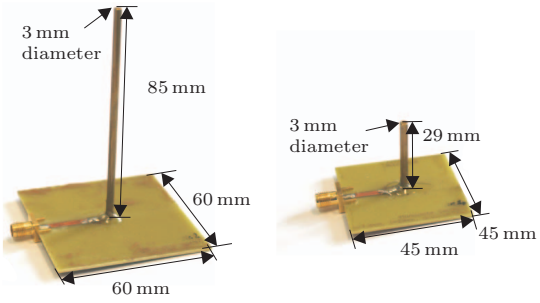

Figure 2. On-body monopole antennas resonant at 900 MHz (on the left) and 2.45 GHz (on the right)

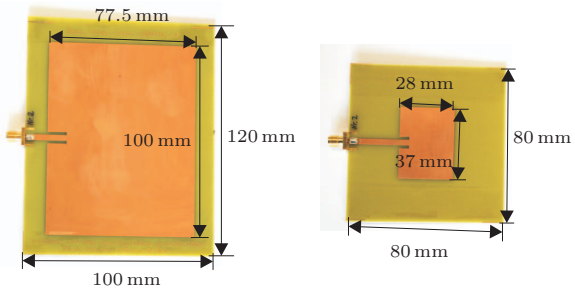

Figure 3. On-body patch antennas resonant at 900 MHz (on the left) and 2.45 GHz (on the right)

III. System Evaluation

The evaluation of the performance of the different RFID systems is done by means of the measured channel transfer functions, S_{21} and S_{12}. The magnitude of the channel transfer function, $|S_{21}|$, defines the channel gain in the forward link of the RFID system, while $|S_{12}|$ defines the channel gain in the backward link.

The cumulative distribution function (CDF) of $|S_{21}|$ directly relates to the outage probability in the system's forward link [21], more precisely to the probability that the backscatter system operates at its limit. The outage probability in the system's forward link is defined as [22]

$$P_{\mathrm{F}} = \mathrm{P}\{|S_{21}|^2 \leq F_{\mathrm{Th}}\}. \tag{1}$$

The threshold, F_{Th}, is defined as the channel gain, which is necessary to realize a chip power equal to the tag's sensitivity, T_{Tag}:

$$F_{\mathrm{Th}} = \frac{T_{\mathrm{Tag}}}{\tau P_{\mathrm{TX,Reader}}}. \tag{2}$$

τ is the power transmission coefficient in the tag and $P_{\mathrm{TX,Reader}}$ is the transmitter (TX) output power of the reader.

The CDF of the product of the channel gain in forward link and backward link, $|S_{21}||S_{12}|$, relates to the outage probability in backward link-limited systems [22]:

$$P_{\mathrm{B}} = \mathrm{P}\{|S_{21}|^2|S_{12}|^2 \leq B_{\mathrm{Th}}\}. \tag{3}$$

The threshold, B_{Th}, is the total channel gain of forward and backward link, which is necessary to realize a receiver (RX) power at the reader equal to the RX's sensitivity, $T_{\mathrm{RX,Reader}}$:

$$B_{\mathrm{Th}} = \frac{T_{\mathrm{RX,Reader}}}{\eta P_{\mathrm{TX,Reader}}}. \tag{4}$$

η is the modulation efficiency of the modulated backscatter signal. A maximum modulation efficiency of about 20 % can be achieved in the case of an ideal amplitude-modulated backscatter signal.

In general, the allowed outage probabilities in a system are governed by the application. In the case of a system, which monitors life parameters of patients with life-threatening deceases in clinical care, the outage probabilities should be close to 0 %. While systems used in sports analysis can deal with higher outage probabilities, e.g., 10 %.

A. Forward Link

The figures, Fig. 4, Fig. 5, Fig. 6, and Fig. 7, show the outage probabilities in the forward link, P_{F}, for the respective links of all four on-body systems.

The curves show that links with longer path lengths, e.g., the stomach-back link (see Fig. 4), show higher outage probabilities in comparison to links with shorter distances, e.g, the stomach-chest link (see Fig. 5). Depending on the on-body link, the link geometry and thus the channel gain is influenced by body movements. Thus, on-body links with higher mobility, i.e., trunk-to-limb links, experience a wider range of outage probabilities than trunk-to-trunk links with lower mobility. Consequently, the outage probability curves of the stomach-back and stomach-chest links (see Fig. 4 and Fig. 5) show steeper curves in comparison to the stomach-wrist and stomach-head links (see Fig. 6 and Fig. 7). These phenomena can be observed for both antenna types in both frequency ranges. The same behavior was observed in [15] at 2.45 GHz.

As expected from theory, the outage probabilities at 900 MHz are lower than the probabilities at 2.45 GHz. This is due to an increased energy absorption in human tissues at higher frequencies [20]. Again, this phenomenon can be observed for both antenna types in both frequency regimes, although there are quite some differences in the patch antennas' radiation efficiencies (see Sec. II-A2).

In addition, the probability curves show that the monopoles are indeed a best-case reference for this system arrangement.

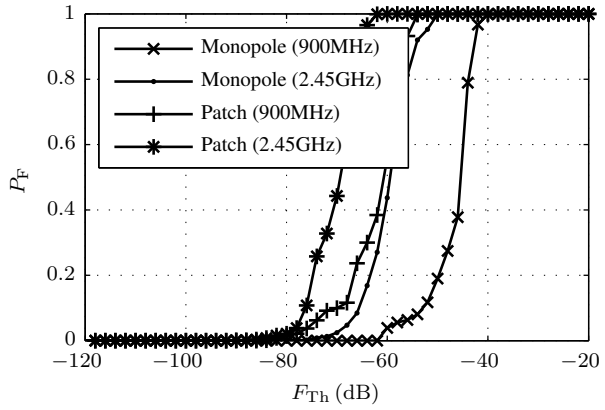

Figure 4. Outage probability, P_F, versus gain threshold, F_{Th}, of the stomach-back link

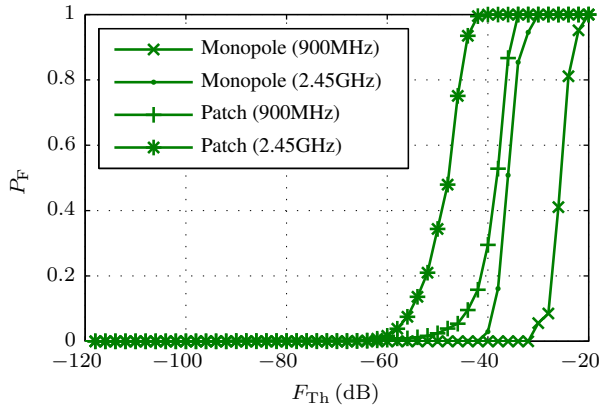

Figure 5. Outage probability, P_F, versus gain threshold, F_{Th}, of the stomach-chest link

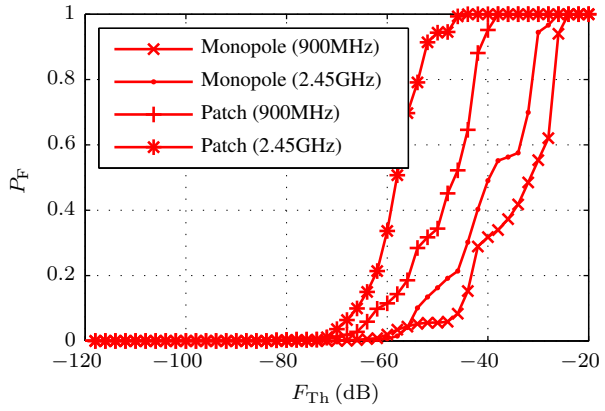

Figure 6. Outage probability, P_F, versus gain threshold, F_{Th}, of the stomach-wrist link

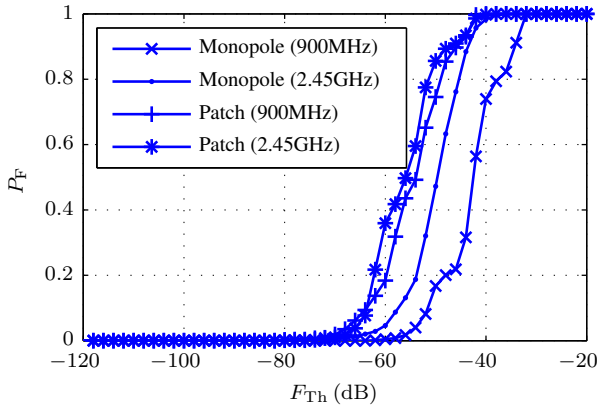

Figure 7. Outage probability, P_F, versus gain threshold, F_{Th}, of the stomach-head link

1) System Example: A modern RFID system provides for example a gain threshold of $F_{Th} = -47\,\mathrm{dB}$ (see Eqn. 2 with $T_{Tag} = -17.8\,\mathrm{dBm}$, $P_{TX,Reader} = 30\,\mathrm{dBm}$, and $\tau = 100\,\%$) [23], [24]. In Tab. I, the outage probabilities of each link and antenna structure are listed for this gain threshold. Tab. I shows that the investigated RFID systems are mostly limited in their forward links. There are different strategies to overcome this limitation. An increase in the TX power at the on-body reader is not an option, because of the safety regulations and power constraints in on-body systems [25], [26]. One possibility is to use semi-passive backscatter tags with chip sensitivities down to $-40\,\mathrm{dBm}$. This sensitivity corresponds to a gain threshold of $F_{Th} = -70\,\mathrm{dB}$. Tab. II shows that semi-passive tags lead to a promising performance in the systems' forward links. However, there is still a rather large limitation in the stomach-back link of the patch antenna systems. This limitation can be resolved by the use of patch antenna realized on a low-loss substrate, or by the use of higher mode patch antennas. Another solution would be the use of a second RFID reader on the person's back to reduce the distance of the propagation path.

B. Backward Link

The figures, Fig. 8, Fig. 9, Fig. 10, and Fig. 11, show the outage probabilities in the backward link, P_B, for the respective on-body links. The same characteristic behavior of on-body links, as described in Sec. III-A, can be observed for the backward links.

1) System Example: Today's RFID systems provide for example a gain threshold of $B_{Th} = -118\,\mathrm{dB}$ (see Eqn. 4 with $T_{RX,Reader} = -95\,\mathrm{dBm}$, $P_{TX,Reader} = 30\,\mathrm{dBm}$, and $\eta = 20\,\%$) [23], [24]. In Tab. III, the outage probabilities of each link and antenna structure are listed for a gain threshold of $B_{Th} = -118\,\mathrm{dB}$. Limitations in the backward links of the systems can be observed. To overcome these, a phase-modulated backscatter signal could be used [4]. This

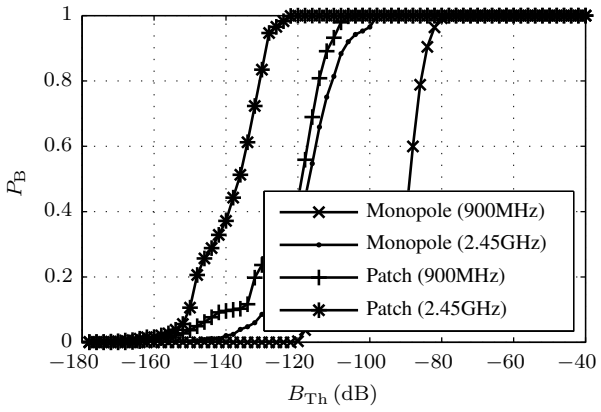

Figure 8. Outage probability, P_{B}, versus gain threshold, B_{Th}, of the stomach-back backward link

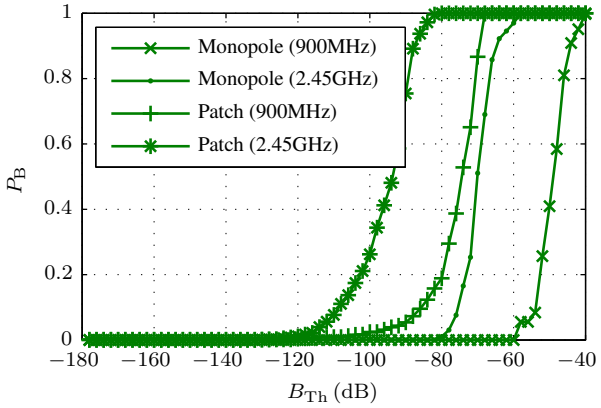

Figure 9. Outage probability, P_{B}, versus gain threshold, B_{Th}, of the stomach-chest backward link

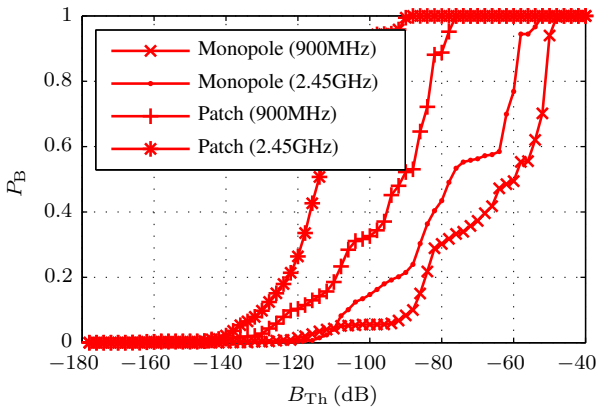

Figure 10. Outage probability, P_{B}, versus gain threshold, B_{Th}, of the stomach-wrist backward link

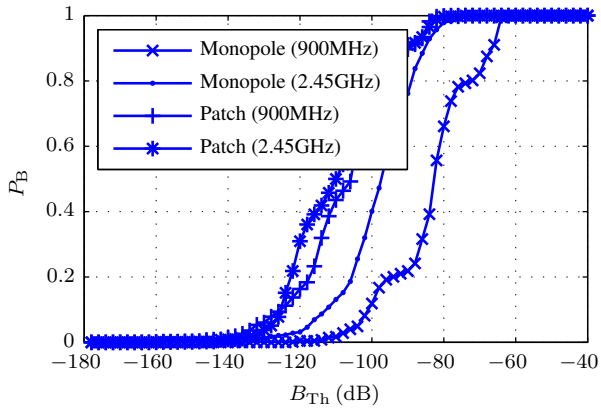

Figure 11. Outage probability, P_{B}, versus gain threshold, B_{Th}, of the stomach-head backward link

modulation scheme provides a maximum modulation efficiency of $\eta = 100\,\%$, which corresponds to gain threshold of about $-125\,\mathrm{dB}$. Tab. IV lists the corresponding outage probabilities. It can be seen that the $6\,\mathrm{dB}$ difference in the threshold, B_{Th}, sufficiently improves the performance in the stomach-chest, stomach-wrist, and stomach-head links. For a further performance enhancement of the systems' stomach-back link, again, a second reader could be used. Other strategies to overcome backward link limitations are, e.g., to realize more suitable antennas or to use a reader RX with a lower sensitivity.

IV. Conclusions

This contribution presents a performance evaluation of on-body RFID systems at $900\,\mathrm{MHz}$ and $2.45\,\mathrm{GHz}$. The evaluation is based on channel transfer function measurements, which were performed in an indoor environment versus standing, sitting, and walking body postures.

Custom-built monopoles and patch antennas are used as on-body antennas. It is found that the monopole antennas give an upper bound for the performance of practical system implementations.

From the channel measurements, the outage probabilities in the forward and backward link of the on-body RFID systems are derived. By evaluating these probabilities, the reliability of the systems is found, limitations in the backscatter communication are identified, and different strategies for an improvement in system performance are suggested. Ultimately, the presented evaluation allows to realize reliable on-body RFID systems.

Table I
OUTAGE PROBABILITIES FOR A GAIN THRESHOLD OF $F_{\mathrm{Th}} = -47\,\mathrm{dB}$

Monopoles	**Back**	**Chest**	**Wrist**	**Head**
900 MHz	30 %	0 %	6 %	21 %
2.45 GHz	100 %	0 %	20 %	64 %
Patch antennas	**Back**	**Chest**	**Wrist**	**Head**
900 MHz	100 %	40 %	46 %	86 %
2.45 GHz	100 %	50 %	95 %	90 %

Table II
OUTAGE PROBABILITIES FOR A GAIN THRESHOLD OF $F_{\mathrm{Th}} = -70\,\mathrm{dB}$

Monopoles	**Back**	**Chest**	**Wrist**	**Head**
900 MHz	0 %	0 %	0 %	0 %
2.45 GHz	2 %	0 %	0 %	0 %
Patch antennas	**Back**	**Chest**	**Wrist**	**Head**
900 MHz	10 %	0 %	2 %	2 %
2.45 GHz	44 %	0 %	4 %	1 %

Table III
OUTAGE PROBABILITIES FOR A GAIN THRESHOLD OF $B_{\mathrm{Th}} = -118\,\mathrm{dB}$

Monopoles	**Back**	**Chest**	**Wrist**	**Head**
900 MHz	4 %	0 %	2 %	1 %
2.45 GHz	44 %	0 %	1 %	5 %
Patch antennas	**Back**	**Chest**	**Wrist**	**Head**
900 MHz	56 %	1 %	12 %	18 %
2.45 GHz	100 %	2 %	34 %	36 %

Table IV
OUTAGE PROBABILITIES FOR A GAIN THRESHOLD OF $B_{\mathrm{Th}} = -125\,\mathrm{dB}$

Monopoles	**Back**	**Chest**	**Wrist**	**Head**
900 MHz	0 %	0 %	1 %	0 %
2.45 GHz	17 %	0 %	1 %	2 %
Patch antennas	**Back**	**Chest**	**Wrist**	**Head**
900 MHz	30 %	0 %	6 %	10 %
2.45 GHz	97 %	0 %	16 %	8 %

ACKNOWLEDGEMENTS

This work was performed as part of the project "MAS – Nanoelectronics for Mobile Ambient Assisted Living-Systems", which is funded by "ENIAC Joint Undertaking" and Austria's "Österreichische Forschungsförderungsgesellschaft".

REFERENCES

[1] Y. Hao and R. Foster, "Wireless Body Sensor Networks for Health-Monitoring Applications," *Physiol. Meas.*, vol. 29, no. 11, pp. R27–R56, November 2008.

[2] S. Patel, H. Park, P. Bonato, L. Chan, and M. Rodgers, "A Review of Wearable Sensors and Systems with Application in Rehabilitation," *Journal of NeuroEngineering and Rehabilitation*, vol. 9, no. 21, pp. 1–17, April 2012.

[3] J. Grosinger and A. Scholtz, "Antennas and Wave Propagation in Novel Wireless Sensing Applications Based on Passive UHF RFID," *e&i Elektrotechnik und Informationstechnik*, vol. 128, no. 11-12, pp. 408–414, 2011.

[4] J.-P. Curty, M. Declercq, C. Dehollain, and N. Joehl, *Design and Optimization of Passive UHF RFID Systems*. New York: Springer Science+Business Media, LLC, 2007.

[5] A. Sample, D. Yaeger, P. Powledge, A. Mamishev, and J. Smith, "Design of an RFID-Based Battery-Free Programmable Sensing Platform," *IEEE Trans. Instrum. Meas.*, vol. 57, no. 11, pp. 2608–2615, November 2008.

[6] G. Marrocco, "Multiport Sensor RFIDs for Wireless Passive Sensing of Objects - Basic Theory and Early Results," *IEEE Trans. Antennas Propag.*, vol. 56, no. 8, pp. 2691–2702, August 2008.

[7] J. Grosinger and J. Griffin, "A Bend Transducer for Backscatter RFID Sensors," in *Proc. IEEE Antennas and Propagation Society International Symposium*, July 2012.

[8] P. Nikitin and K. Rao, "Performance Limitations of Passive UHF RFID Systems," in *Proc. IEEE Antennas and Propagation Society International Symposium*, July 2006.

[9] A. Sani, M. Rajab, R. Foster, and Y. Hao, "Antennas and Propagation of Implanted RFIDs for Pervasive Healthcare Applications," *Proc. IEEE*, vol. 98, no. 9, pp. 1648–1655, September 2010.

[10] C. Schmidt, D. Valderas, J. Garcia, I. Ortego, and X. Chen, "Passive UHF RFID Near Field Link Budget for Implanted Sensors," in *Proc. European Conference on Antennas and Propagation*, April 2011.

[11] C. Occhiuzzi, G.Contri, and G. Marrocco, "Design of Implanted RFID Tags for Passive Sensing of Human Body: the STENTag," *IEEE Trans. Antennas Propag.*, vol. 60, no. 7, pp. 3146–3154, July 2012.

[12] M. Polivka, M. Svanda, P. Hudec, and S. Zvanovec, "UHF RF Identification of People in Indoor and Open Areas," *IEEE Trans. Microw. Theory Tech.*, vol. 57, no. 5, pp. 1341–1347, May 2009.

[13] C. Occhiuzzi, S. Cippitelli, and G. Marrocco, "Modeling, Design and Experimentation of Wearable RFID Sensor Tag," *IEEE Trans. Antennas Propag.*, vol. 58, no. 8, pp. 2490–2498, August 2010.

[14] S. Cotton, W. Cully, W. Scanlon, and J. McQuiston, "Channel Characterisation for Indoor Wearable Active RFID at 868 MHz," in *Proc. Loughborough Antennas and Propagation Conference*, November 2011.

[15] P. Hall and Y. Hao, *Antennas and Propagation for Body-Centric Wireless Communications*. USA: Artech House, INC., 2006.

[16] S. Manzari, C. Occhiuzzi, and G. Marrocco, "Body-Centric RFID Systems," in *Proc. International Symposium on Applied Sciences in Biomedical and Communication Technologies*, October 2011.

[17] G. Conway and W. Scalon, "Antennas for Over-Body-Surface Communication at 2.45 GHz," *IEEE Trans. Antennas Propag.*, vol. 57, no. 4, pp. 844–855, April 2009.

[18] P. Hall, Y. Hao, Y. Nechayev, A. Alomainy, C. Constantinou, C. Parini, M. Kamarudin, T. Salim, D. Hee, R. Dubrovka, A. Owadally, W. Song, A. Serra, P. Nepa, M. Gallo, and M. Bozzetti, "Antennas and Propagation for On-Body Communication Systems," *IEEE Antennas Propag. Mag.*, vol. 49, no. 3, pp. 41–58, June 2007.

[19] J. Grosinger and M. Fischer, "Indoor On-Body Channel Measurements at 900 MHz," in *Proc. IEEE-APS Topical Conference on Antennas and Propagation in Wireless Communications*, September 2011.

[20] S. Gabriel, R. Lau, and C. Gabriel, "The Dielectric Properties of Biological Tissue: III. Parametric Models for the Dielectric Spectrum of Tissues," *Phys. Med. Biol.*, vol. 41, no. 11, pp. 2271–2293, November 1996.

[21] G. Lasser, R. Langwieser, F. Xaver, and C. Mecklenbräuker, "Dual-Band Channel Gain Statistics for Dual-Antenna Tyre Pressure Monitoring RFID Tags," in *Proc. IEEE International Conference on RFID*, April 2011.

[22] J. Grosinger, "Backscatter Radio Frequency Systems and Devices for Novel Wireless Sensing Applications," Ph.D. dissertation, Vienna University of Technology, 2012.

[23] Impinj, Inc. (2012, May) Indy R1000 Reader Chip (IPJ-P1000). [Online]. Available: http://www.impinj.com

[24] ——. (2012, May) Monza 5 Tag Chip Datasheet (IPJ-W1600). [Online]. Available: http://www.impinj.com

[25] "Guidelines for Limiting Exposure to Time-Varying Electric, Magnetic, and Electromagnetic Fields (Up to 300 GHz)," *Health Phys*, vol. 74, no. 4, pp. 494–522, April 1998.

[26] "IEEE Standard for Safety Levels with Respect to Human Exposure to Radio Frequency Electromagnetic Fields, 3 kHz to 300 GHz," *IEEE Std C95.1-1991*, 1992.